

# Equilibria and dynamics in binary and ternary uranyl oxalate and acetate/fluoride complexes†

Wenche Aas, Zoltán Szabó and Ingmar Grenthe\*

*Inorganic Chemistry, Department of Chemistry, Royal Institute of Technology (KTH), S-100 44, Stockholm, Sweden. E-mail: ingmarg@inorg.kth.se; Fax: +46-8-21 26 26*

*Received 30th October 1998, Accepted 16th February 1999*

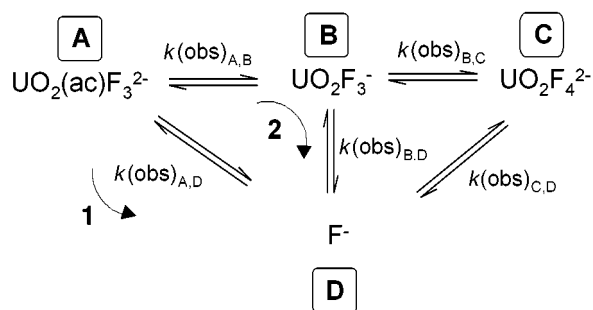
The formation of ternary  $\text{UO}_2(\text{ac})_p\text{F}_q^{2-p-q}$  ( $p = 1$  or  $2$  and  $q = 1-3$ ) complexes, and their equilibrium constants were investigated by potentiometric titrations and  $^{19}\text{F}$  NMR spectroscopy. The equilibrium constants have been determined from the emf data in a  $\text{NaClO}_4$  medium at constant sodium concentration,  $[\text{Na}^+] = 1.00 \text{ M}$  at  $25^\circ\text{C}$ , except for the  $\text{UO}_2(\text{ac})\text{F}_3^{2-}$  complex where  $^{19}\text{F}$  NMR at  $-5^\circ\text{C}$  was used. The magnitude of the equilibrium constant for the stepwise addition of fluoride indicates that prior co-ordination of acetate has only a small effect on the subsequent bonding of fluoride. The acetate exchange in the ternary  $\text{UO}_2(\text{ac})\text{F}_3^{2-}$  complex was studied using  $^{19}\text{F}$  NMR. Through magnetisation transfer experiments, it was possible to confirm the provisional mechanism from a previous study and also the consistency of the rate constants for the five different exchange pathways required to describe the fluoride exchange. The exchange takes place *via* the intermediate  $\text{UO}_2\text{F}_3(\text{H}_2\text{O})_2^-$ , indicating that the acetate exchange follows an interchange mechanism with solvent participation in the transition state. The rates and mechanisms of the ligand exchange reactions in  $\text{UO}_2(\text{ox})_2(\text{H}_2\text{O})^{2-}$  and  $\text{UO}_2(\text{ac})_2(\text{H}_2\text{O})$  have been studied using  $^{13}\text{C}$  NMR techniques at  $-5^\circ\text{C}$ . The rate law is  $v = k[\text{complex}][\text{ligand}]$ , and the second order rate constant and the activation parameters for both systems have been determined. The reactions most likely take place through an Eigen–Wilkins type of mechanism, where the first step is a pre-equilibrium of an outer-sphere complex followed by a rate determining exchange of water. The rate constants for the water exchange reactions are very similar to that in  $\text{UO}_2(\text{H}_2\text{O})_9^{2+}$ . The information from the binary oxalate system rules out the formation of  $\text{UO}_2(\text{ox})_2(\text{H}_2\text{O})^{2-}$  as an intermediate in the exchange reactions in the previously studied  $\text{UO}_2(\text{ox})_2\text{F}_3^{3-}$ , also in this case confirming a previously suggested exchange mechanism. The  $\text{H}^+/\text{D}^+$  isotope effects and a linear free energy relationship suggest that the main catalytic effect of  $\text{H}^+$  on ligand exchange rates is due to the formation of a protonated precursor. Hence, the catalytic effect depends on the basicity of the ligand and the site for the proton attack.

## Introduction

In earlier studies,<sup>1–3</sup> we have discussed the rates and mechanisms of ligand exchange reactions in binary  $\text{U}^{\text{VI}}$ –fluoride<sup>1</sup> and ternary  $\text{UO}_2\text{L}_p\text{F}_q$  systems<sup>2,3</sup> where L is picolinate (pyridine-2-carboxylate), oxalate or carbonate. The fluoride exchange in the binary uranyl–fluoride system<sup>1</sup> is consistent with a concerted Eigen–Wilkins mechanism, at least as long as water is present in the co-ordination sphere. The rate constant for the exchange decreases by approximately three orders of magnitude when all water molecules are replaced by fluoride<sup>1,4</sup> as in  $\text{UO}_2\text{F}_5^{3-}$ , or by a bidentate ligand as in  $\text{UO}_2\text{LF}_3$  and  $\text{UO}_2\text{L}_2\text{F}$  where L is carbonate, oxalate or picolinate.<sup>2</sup> In a separate determination of the equilibrium constants in the ternary systems we showed that the stepwise binding constants of fluoride are remarkably little influenced by the presence of other strongly bonded ligands.<sup>5</sup> The same is valid for the ligand exchange mechanism as discussed in some detail in a previous study.<sup>3</sup> Both the fluoride and L exchanges are proton catalysed, and we have used this fact, together with determinations of H/D isotope effects, to obtain additional information on the intimate mechanisms of these reactions. An important point in the previous study was to decide the extent of water involvement in the intra- and inter-molecular ligand exchange reactions.<sup>3</sup> In this context we identified “ $\text{UO}_2\text{F}_3$ ” as a transition state/intermediate in the

carbonate and 4-nitropicolinate exchange reactions of  $\text{UO}_2\text{LF}_3$  complexes, where “ $\text{UO}_2\text{F}_3$ ” is not identical with  $\text{UO}_2(\text{H}_2\text{O})_2\text{F}_3^-$  but contains a lower number of co-ordinated waters. This is a strong indication of a dissociative exchange mechanism. We have previously made some experimental observations of ligand exchange in the ternary  $\text{UO}_2(\text{ac})\text{F}_3^{2-}$  system<sup>2</sup> and found that the intermolecular fluoride exchange has a rate constant of 40 to 50  $\text{s}^{-1}$ , which is about 4 times faster than in the other ternary systems. The intramolecular exchange is much faster, as judged from the line broadening of about 700 Hz of the NMR signals from the co-ordinated fluorides. This is due to fast acetate exchange, which results in fast site exchange between the fluorides. The estimated rate is about two orders of magnitude faster than that of the other L ligands studied. As it was not possible to make a direct study of the exchange of acetate in the ternary system, we have made additional measurements to corroborate the previous results and to obtain further mechanistic insights. The present study consists of two parts, the first a determination of equilibrium constants in the ternary  $\text{U}^{\text{VI}}$ –acetate–fluoride system, using potentiometry and  $^{19}\text{F}$  NMR methodology, the second part a study of the exchange mechanism and the consistency of our experimental data in more detail. This was done by the use of magnetisation transfer to obtain more precise rate constants and to establish the coupling between the different exchange pathways in Scheme 1. We have also studied the ligand exchange reactions in the binary acetate and oxalate systems in order to decide if water is involved in the ligand exchange, or not. The information for the binary oxalate system was used to corroborate previous conclusions on the ligand exchange mechanisms in the ternary uranium(VI)–oxalate–fluoride system.

† Supplementary data available: exchange rate dependences, species distributions, NMR spectra. For direct electronic access see <http://www.rsc.org/suppdata/dt/1999/1311/>, otherwise available from BLDSC (No. SUP 57505, 8 pp.) or the RSC Library. See Instructions for Authors, 1999, Issue 1 (<http://www.rsc.org/dalton>).



Scheme 1

The experimental methodology involves dynamic NMR studies using  $^{19}\text{F}$  and  $^{13}\text{C}$  NMR methods. In addition we have used the NMR data to confirm and in one case to determine equilibrium constants in the ternary acetate system.

## Experimental

### Solutions

Stock solutions of uranium(vi) perchlorate and perchloric acid were prepared as described elsewhere.<sup>6</sup> The sodium perchlorate was prepared from  $\text{NaClO}_4 \cdot \text{H}_2\text{O}$  (analytical grade) and analysed by weighing samples dried at  $120^\circ\text{C}$ . Sodium fluoride, sodium oxalate and sodium acetate were all of analytical grade. The nitrogen gas used for stirring of the test solutions was purified by successively passing it through 10% NaOH, 10%  $\text{H}_2\text{SO}_4$ , 1 M  $\text{NaClO}_4$  and a G4 filter. Perchloric acid and NaOH were used to adjust the pH in the preparation of the NMR solutions. The  $^{13}\text{C}$  NMR measurements were made using  $^{13}\text{C}$ -enriched  $\text{Na}(\text{CH}_3^*\text{CO}_2)$  (Campro Science 99%  $^{13}\text{C}$ ) and  $^{13}\text{C}$ -enriched  $\text{Na}_2\text{C}_2\text{O}_4$  (Isotec Inc. 99.2%  $^{13}\text{C}$ ).

### Potentiometric titrations in the uranyl(vi)–acetate–fluoride system

All emf measurements were performed in a thermostatted box at  $25.00 \pm 0.05^\circ\text{C}$  and monitored by an automated computer system. The criterion for equilibrium was that the emf should remain constant within  $0.1 \text{ mV h}^{-1}$ , which took 20–30 min after each addition of titrant. The fluoride (6.0502.150) and reference (Ag–AgCl, 6.0726.100) electrodes were from Metrohm. The hydrogen ion concentration ( $-\log [\text{H}^+]$ ) was measured by a HF resistant combined glass electrode from Ingold (HF-405-60-57/120), where the inner solution of KCl was replaced by 1 M NaCl to avoid precipitation of  $\text{KClO}_4$  in the liquid junction. The pH was measured using a pH meter from Orion (model 210A), and  $[\text{H}^+]$  was calculated and corrected for the “Irving factor”<sup>7</sup> in the working media. All titrations were performed in Teflon vessels using a  $\text{NaClO}_4$  medium at constant sodium concentration,  $[\text{Na}^+] = 1.00 \text{ M}$ . The methodology used requires fairly large variations in the perchlorate concentrations between the different titration series as will be discussed later.

In the experiments the total uranyl and acetate concentrations were kept constant, while the fluoride concentration was varied. The fluoride membrane electrode was calibrated in the sodium perchlorate/acetate media before the experiment, using a standard NaF solution.<sup>8</sup> The uranyl:acetate ratio was varied in the different experiments. The pH was kept almost constant at *ca.* 4.7, which is in the region where the buffer capacity of the system is largest. There was no need to take the formation of HF at this pH into account, and the average number of fluorides bonded to uranyl is accordingly  $\bar{n}_\text{F} = ([\text{F}^-]_\text{total} - [\text{F}^-])/[\text{UO}_2^{2+}]_\text{total}$ . The equilibrium constants were calculated and refined with the LETAGROP<sup>9</sup> least squares program, using the total fluoride concentrations as the error-carrying variable. All experimental points were given unit

weight in the least-squares refinement. Hence, we had to use approximately the same number of experimental points in the regions where the different complexes were predominant.

### NMR Measurements

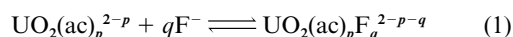
The NMR spectra were recorded on Bruker AM400 and DMX500 spectrometers at  $-5^\circ\text{C}$ , unless otherwise mentioned and 5%  $\text{D}_2\text{O}$  solutions were used to obtain locked mode. The temperatures were checked using the chemical shifts of methanol.<sup>10</sup> The test solutions were measured in 5 (for  $^{19}\text{F}$ ) or 10 mm (for  $^{13}\text{C}$ ) NMR tubes. The  $^{19}\text{F}$  NMR spectra were recorded at 376.4 or 470.5 MHz and  $25^\circ\text{C}$  using an aqueous solution of 0.01 M NaF in 1 M  $\text{NaClO}_4$  (pH 12) as reference,  $^{13}\text{C}$  NMR spectra (125.7 MHz) at  $25^\circ\text{C}$  and referenced to the methyl signal of sodium 3-(trimethylsilyl)propionate- $\text{d}_4$ . The linewidths were determined by fitting a Lorentzian curve to the experimental signal using the standard Bruker software. Selective inversion transfer experiments were performed using Gaussian pulses. The ligand exchange reactions were studied using different dynamic NMR methods that are well documented; we have<sup>1,2,11</sup> given a summary of them.

The uncertainty estimated for the rate constants and activation parameters is given as  $1\sigma$ , for the formation constants calculated with the LETAGROP program as  $3\sigma$ .

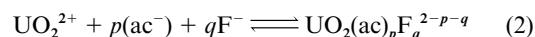
## Results and discussion

### Constitution

The stoichiometry and equilibrium constants of the different complexes were determined using potentiometric and  $^{19}\text{F}$  NMR techniques. The titrations had to be carried out at high acetate concentrations due to the weak complexes formed.<sup>12</sup> The free acetate concentration is therefore near constant throughout the experiments and when interpreting the experimental data the system can in the first approximation be considered as a binary system, eqn. (1). The titration curves (Fig. 1) for three different



total concentrations of uranium almost coincide, indicating that no polynuclear species are formed and that the equilibria at each total concentration of acetate can be described with a set of conditional equilibrium constants. In order to calculate the equilibrium constants from the components, eqn. (2), we used



data for the protonation constant of acetate and the formation constants for the binary uranyl–acetate<sup>12</sup> and uranyl–fluoride systems<sup>13</sup> taken from the literature. The chemical model was then tested and refined by a least-squares refinement using 148 experimental data. The best model included five different ternary species, four of which were also identified by  $^{19}\text{F}$  NMR, except  $\text{UO}_2(\text{ac})\text{F}$ , which coincide with  $\text{UO}_2(\text{ac})_2\text{F}^-$ . One set of NMR data and the corresponding distribution diagram are shown in SUP 57505. The potentiometric titrations are less precise at high concentrations of free fluoride due to the small difference between  $[\text{F}^-]_\text{total}$  and  $[\text{F}^-]$ , and were therefore interrupted at  $\bar{n}_\text{F}$  around two, where at most 5% of the limiting complex  $\text{UO}_2(\text{ac})\text{F}_3^{2-}$  was present. A more precise value of the equilibrium constant,  $\log \beta_{13} = 11.7 \pm 0.1$ , for this species was obtained from the integrals of  $\text{F}^-$ ,  $\text{UO}_2(\text{ac})\text{F}_3^{2-}$  and  $\text{UO}_2\text{F}_3^-$  using  $^{19}\text{F}$  NMR at  $-5^\circ\text{C}$ . This is very different from the value  $11.13 \pm 0.09$  obtained from the titration data, indicating that great care has to be used before accepting the numerical value of equilibrium constants of species present in small amounts. For the other complexes the agreement between the equilibrium constants determined by potentiometry and using NMR data was within the experimental uncertainty. In order to combine

**Table 1** Equilibrium constants,  $\log \beta_{pq}$ , for the reactions  $\text{UO}_2^{2+} + p(\text{ac}) + q\text{F}^- \rightleftharpoons \text{UO}_2(\text{ac})_p\text{F}_q$  determined in a 1.00 M  $\text{NaClO}_4$  ionic medium at 25 °C. The uncertainty is equal to three times the estimated standard deviation in the least-squares refinement of the experimental data

Complex	$\log \beta$	Stepwise F	Stepwise ac
$\text{UO}_2(\text{ac})\text{F}$	$6.66 \pm 0.14$	4.24 (4.46)	2.12 (2.34)
$\text{UO}_2(\text{ac})\text{F}_2^-$	$9.63 \pm 0.04$	2.97 (3.27)	1.65 (2.04)
$\text{UO}_2(\text{ac})\text{F}_3^{2-}$	$11.70 \pm 0.10$	2.07 (2.55)	1.29 (1.99)
$\text{UO}_2(\text{ac})\text{F}_2^{2-}$	$7.65 \pm 0.09$	3.23 (3.93)	0.99 (1.29)
$\text{UO}_2(\text{ac})_2\text{F}_2^{2-}$	$10.15 \pm 0.05$	2.50 (3.10)	0.52 (0.92)

Data from  $^{19}\text{F}$  NMR experiments at -5 °C. The figures in italics are the stepwise equilibrium constants. The stepwise equilibrium constants,  $\log K_{q+1}$ , for the reactions  $\text{UO}_2\text{F}_q^{2-q} + \text{F}^- \rightleftharpoons \text{UO}_2\text{F}_{q+1}^{1-q}$ ,  $q = 0$  to 2, from the literature<sup>13</sup> are equal to 4.54, 3.44 and 2.43, respectively, and for the reactions  $\text{UO}_2(\text{ac})_p^{2-p} + \text{ac}^- \rightleftharpoons \text{UO}_2(\text{ac})_{p+1}^{1-p}$ ,  $p = 0$ –2, are 2.42, 2.00 and 1.98.<sup>12</sup> The values in parentheses were obtained when taking the statistical factor into account.

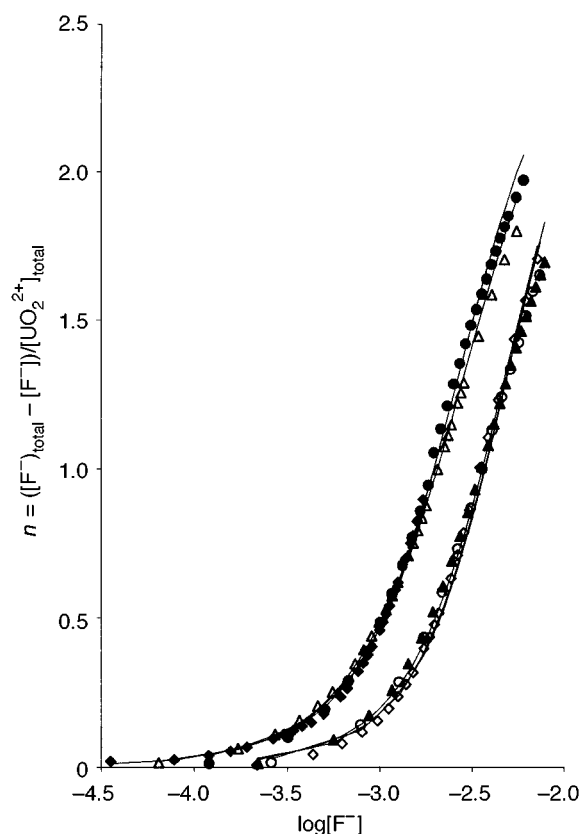
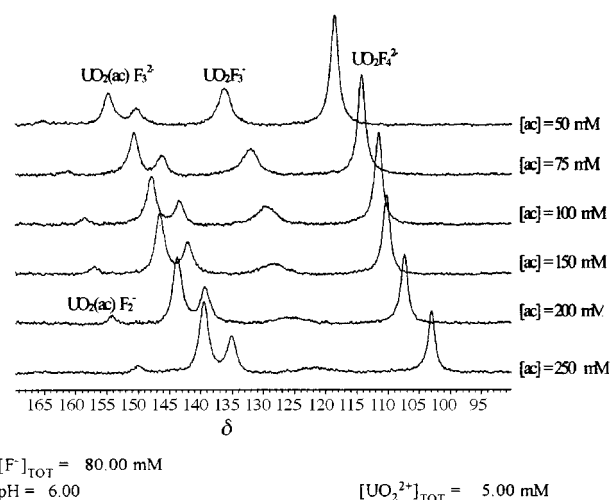


**Fig. 1** Titration curves for the ternary  $\text{UO}_2(\text{ac})_p\text{F}_q$  system. The solid lines are the theoretical curves calculated from the equilibrium constants in Table 1.  $\diamond$ ,  $[\text{UO}_2^{2+}]_{\text{total}} = 2.2$ ,  $[\text{ac}]_{\text{total}} = 200$ ;  $\blacktriangle$ ,  $[\text{UO}_2^{2+}]_{\text{total}} = 5.7$ ,  $[\text{ac}]_{\text{total}} = 200$ ;  $\circ$ ,  $[\text{UO}_2^{2+}]_{\text{total}} = 11.5$ ,  $[\text{ac}]_{\text{total}} = 200$ ;  $\blacklozenge$ ,  $[\text{UO}_2^{2+}]_{\text{total}} = 2.2$ ,  $[\text{ac}]_{\text{total}} = 400$ ;  $\triangle$ ,  $[\text{UO}_2^{2+}]_{\text{total}} = 5.7$ ,  $[\text{ac}]_{\text{total}} = 400$ ;  $\bullet$ ,  $[\text{UO}_2^{2+}]_{\text{total}} = 11.5$ ,  $[\text{ac}]_{\text{total}} = 400$  mM.

the experimental information from both potentiometric and NMR data, we have chosen to fix  $\log \beta_{13} = 11.7$  in the LETAGROP refinements. Using this value, we obtained a slightly poorer overall fit of the data, the standard deviation in the error-carrying variable (the total fluoride concentration) increasing from 0.15 to 0.24 mM. The least-squares refinement was complicated by correlation between the stability constants for  $\text{UO}_2(\text{ac})\text{F}$  and  $\text{UO}_2(\text{ac})_2\text{F}^-$ . This problem was circumvented by first fitting two constants  $\log \beta_{1q}$  ( $q = 1$  or 2), which were then fixed while the two remaining constants  $\log \beta_{2q}$  ( $q = 1$  or 2) were determined. This procedure was repeated several times until the whole set of stability constants remained unchanged. Using this set we calculated  $-\log [\text{H}^+]$  in the various test solutions and



$[\text{F}^-]_{\text{TOT}} = 80.00 \text{ mM}$   
 $\text{pH} = 6.00$   
 $[\text{UO}_2^{2+}]_{\text{TOT}} = 5.00 \text{ mM}$

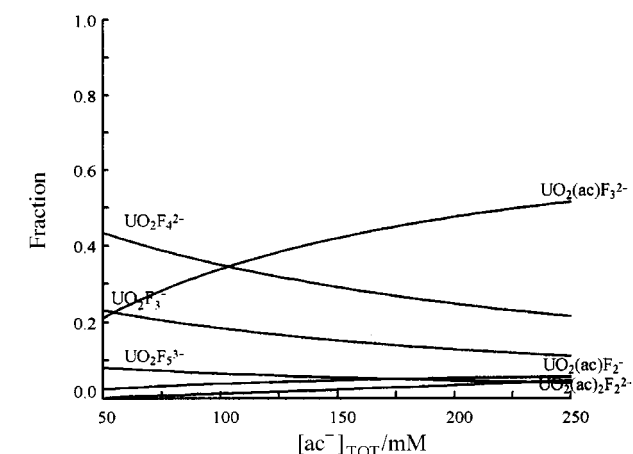


**Fig. 2** The  $^{19}\text{F}$  NMR spectra and the distribution diagram for solutions of  $[\text{UO}_2^{2+}]_{\text{total}} = 5$ ,  $[\text{F}^-]_{\text{total}} = 80$  mM, pH 6 and  $[\text{ac}]_{\text{total}}$  varying from 50 to 250 mM at -5 °C.

found that they agreed with the experimental values, within the experimental uncertainty. The ionic medium has a constant sodium concentration, but the anions are a mixture of  $\text{ClO}_4^-$  and  $\text{ac}^-$  with ratio 4:1 or 3:2. The activity coefficients of the various ionic species may then differ from those in 1.0 M  $\text{NaClO}_4$ , at least for the cations, resulting in slightly different values of the stability constants as compared to those reported in 1.0 M  $\text{NaClO}_4$ . However, the least-squares analysis indicated that this change was not significant. The experimental equilibrium constants given in Table 1 show that the values of the conditional fluoride formation constants are close to the stepwise formation constant in the binary uranyl–fluoride system, especially when the differences in the statistical factor between the binary and ternary systems are taken into account. We made the same observation in the previously studied ternary systems.<sup>5</sup>

It is interesting that  $\text{UO}_2\text{L}_2\text{F}_2$  is formed for  $\text{L} = \text{acetate}$ , but not in the corresponding picolinate, carbonate and oxalate systems. This is certainly related to how the ligand is co-ordinated. In a previous paper<sup>2</sup> we reported two broad  $^{19}\text{F}$  NMR peaks in the ratio 2:1 for the  $\text{UO}_2(\text{ac})\text{F}_3^{2-}$  complex (Fig. 2). This can only arise if it is five-co-ordinated with a symmetric bidentate co-ordination of acetate in the plane perpendicular to the linear “yl” ion. From the stoichiometry alone we cannot decide if both acetate ligands are bidentate also in  $\text{UO}_2(\text{ac})_2\text{F}_2^{2-}$ . The small ligand bite,  $\approx 2.2$  Å, makes such co-ordination possible. The equilibrium constant may indicate whether a ligand forms chelates or not. Stronger complexes are usually formed when the ligands are chelating; however, steric repulsion may decrease the effect. The small stepwise

equilibrium constant,  $\log K = 0.52$ , for the bonding of the second acetate to  $\text{UO}_2(\text{ac})\text{F}_3^{2-}$  may indicate a steric repulsion and/or co-ordination of only one carboxylate oxygen. The fact that  $\text{UO}_2\text{L}_2\text{F}_2$  is not formed by other bidentate ligands, neither those with a larger ligand bite ( $\approx 2.5$  Å in oxalate and picolinate), or with carbonate, indicates a strong preference for five-co-ordination.

### Ligand exchange reactions in the acetate systems

The broad  $^{19}\text{F}$  NMR peaks observed for  $\text{UO}_2(\text{ac})\text{F}_3^{2-}$  indicate a fast fluoride exchange within the co-ordination sphere, and/or between this and free fluoride; however, not so fast that one common peak arises. Magnetisation transfer showed that the direct exchange with free fluoride is slow; hence, the broad fluoride peaks are due to rapid intramolecular fluoride exchange between the two different fluoride sites, which is a result of fast acetate exchange. The direct investigation of acetate exchange by  $^{13}\text{C}$  NMR spectroscopy is not possible in the ternary system because of the large excess of free acetate, compared to the concentration of the complex. In order to obtain additional insight into the mechanism of acetate exchange we studied the rate and mechanism of the acetate exchange between  $\text{UO}_2(\text{ac})_3^-$  and free  $\text{Hac}/\text{ac}^-$ . The crystal structure of this complex shows a bidentate co-ordination of all the acetates with a symmetric six-co-ordination in the equatorial plane of the uranyl ion.<sup>14</sup> The very similar stepwise equilibrium constants<sup>12</sup> indicate six-co-ordination in solution as well.

**In the ternary  $\text{UO}_2(\text{ac})\text{F}_3^{2-}$  complex.** In a previous paper,<sup>2</sup> we have demonstrated that the exchange reactions of L and F follow separate pathways for the complexes  $\text{UO}_2\text{LF}_3$ , where L is oxalate, carbonate and various picolinate. The exchange of these bidentate ligands is 2 or 3 times slower than that of fluoride, with the exception of the weaker co-ordinated 4-nitropicolinate. The exchange reactions in the acetate system also follow two parallel pathways, but differ from the other ternary systems because the L exchange is approximately two orders of magnitude faster than that of fluoride, resulting in the formation of the intermediate/transition state “ $\text{UO}_2\text{F}_3$ ”. The state of hydration of this species is of key importance when deciding if the exchange reaction follows an associative or a dissociative mechanism. From the equilibrium constants, cf. Table 1, one finds that it is not possible to prepare test solutions containing only  $\text{UO}_2(\text{ac})\text{F}_3^{2-}$  and free acetate, other complexes are always present. Owing to the high acetate concentration, the rate of exchange of acetate can only be determined indirectly from the inter- and intra-molecular fluoride exchanges, either from the line broadening or in magnetisation transfer experiments between free fluoride and the complexes.

In a test solution containing 5 mM  $\text{U}^{\text{VI}}$ , 50 mM fluoride and 100 mM acetate at pH 8.2 in addition to free fluoride the dominant complexes are  $\text{UO}_2(\text{ac})\text{F}_3^{2-}$ ,  $\text{UO}_2\text{F}_3^-$  and  $\text{UO}_2\text{F}_4^{2-}$ . Scheme 1 shows the exchange reactions in this system and their corresponding pseudo first order rate constants. They were used as a model in a rate matrix for the evaluation of the magnetisation transfer experiment. By inverting the free fluoride signal, we found that the time dependence of the signal intensities of the complexes was very similar. This is a clear indication of a fast equilibrium, which equalises the transferred negative magnetisation between the complexes. From the known rate constants ( $k_{3,\text{F}}$ ,  $k_{4,\text{F}}$  and  $k_{3,4}$  are defined in a previous study<sup>1</sup>) the pseudo first order rate constants for the binary complexes  $\{k(\text{obs})_{\text{B,D}} = 2k_{3,\text{F}}[\text{F}], k(\text{obs})_{\text{C,D}} = 2k_{4,\text{F}}[\text{F}] \text{ and } k(\text{obs})_{\text{B,C}} = 2k_{3,4}[\text{UO}_2\text{F}_4^{2-}]\}$  can be calculated. In Scheme 1, 1 and 2 indicate two different fluoride exchange pathways for  $\text{UO}_2(\text{ac})\text{F}_3^{2-}$ . Since the rate constant for pathway 1,  $k(\text{obs})_{\text{A,D}}$ , in the previously investigated ternary complexes was nearly independent of L, and approximately equal to  $15 \text{ s}^{-1}$ , the same value was

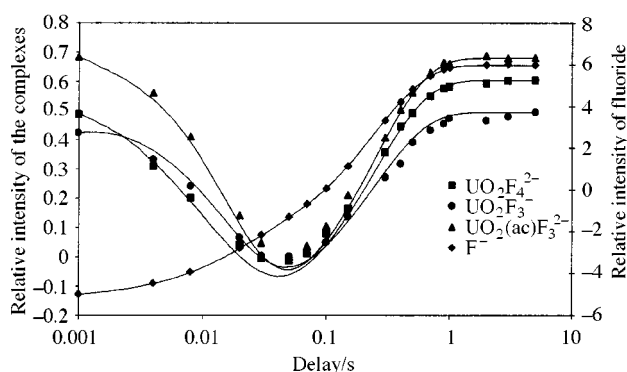
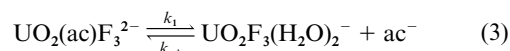


**Fig. 3** Experimental data from the magnetisation transfer experiment made by a selective inversion of the free fluoride peak. The solid lines were obtained by using the model in Scheme 1 and previously determined rate constants.

used in the model together with the acetate dissociation rate,  $k(\text{obs})_{\text{A,B}} = 2000 \text{ s}^{-1}$  (pathway 2), calculated from the linewidth (see below). Using Scheme 1 and the previously determined rate constants, we can now calculate the rate of magnetisation transfer. The agreement between the measured points and the calculated curves is excellent, cf. Fig. 3, which indicates the consistency of the experimental results. The experiment also shows that the intermolecular exchange of fluoride between  $\text{UO}_2(\text{ac})\text{F}_3^{2-}$  and free fluoride takes place *via* two pathways, a direct exchange by fluoride dissociation as in the other ternary systems and a second pathway by the acetate dissociation. It also strongly indicates that the intermediate/transition state for the acetate exchange is identical with the binary  $\text{UO}_2\text{F}_3(\text{H}_2\text{O})_2^-$  complex. In the corresponding carbonate system we have shown that “ $\text{UO}_2\text{F}_3^-$ ” contains less co-ordinated water. The acetate exchange reaction can now be written as in eqn. (3).



If the reverse reaction in eqn. (3) follows a second order rate law *via* the  $\text{UO}_2\text{F}_3(\text{H}_2\text{O})_2^-$  complex as indicated, the fluoride linewidth should depend on the equilibrium concentration of free acetate. To test this we varied the free acetate concentration and measured the linewidths in the  $^{19}\text{F}$  NMR spectra. Fig. 2 clearly indicates that the line broadening of  $\text{UO}_2\text{F}_3^-$  varies with the acetate concentration, which shows unambiguously that  $\text{UO}_2\text{F}_3(\text{H}_2\text{O})_2^-$  is a reactant in eqn. (3). Hence, the acetate exchange follows an interchange mechanism, with bonding of the entering water ligand in the transition state. This is in contrast to the carbonate system, which follows a dissociative exchange mechanism with the unsaturated “ $\text{UO}_2\text{F}_3^-$ ” as intermediate/transition state.<sup>3</sup>

For the quantitative evaluation of the  $^{19}\text{F}$  line broadening of  $\text{UO}_2\text{F}_3^-$  two other reactions have to be taken into account as in the magnetisation transfer experiment, the rate constants for external fluoride exchange ( $k_{3,\text{F}}$ ) and the exchange with  $\text{UO}_2\text{F}_4^{2-}$  ( $k_{3,4}$ ), which are known. The rate constant, calculated from the linewidth of the  $\text{UO}_2\text{F}_3^-$  peak, is then the sum of those of three exchange reactions, eqn. (4), where the factor 2

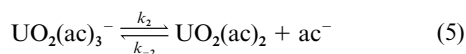
$$k_{\text{obs}} = k_{-1}[\text{ac}] + 2k_{3,\text{F}}[\text{F}] + 2k_{3,4}[\text{UO}_2\text{F}_4^{2-}] \quad (4)$$

takes the reverse reactions into account. By a non-linear least-squares fitting, using the previously determined values of  $k_{3,\text{F}}$  and  $k_{3,4}$  and the calculated equilibrium concentrations (SUP 57505), we obtained  $k_{-1} = (2.5 \pm 0.1) \times 10^4 \text{ M}^{-1} \text{ s}^{-1}$ . This value is not strongly dependent on the values of  $k_{3,\text{F}}$  and  $k_{3,4}$ , indicating that these reactions make only a minor contribution to the line broadening, this is also seen in SUP 57505, where the experimental data are almost a linear function of the acetate concentration. There is no evidence for a direct acetate

exchange between  $\text{UO}_2(\text{ac})\text{F}_3^{2-}$  and  $\text{UO}_2\text{F}_3^-$ . The acetate dissociation rate constant  $k_1 = 1300 \text{ s}^{-1}$  was calculated from the equilibrium constant for reaction (3), given in Table 1. The largest source of uncertainty in  $k_1$  is the error in the equilibrium constant, which corresponds to approximately  $400 \text{ s}^{-1}$  in the rate constant. This may be the reason why the value is smaller than that ( $2050 \text{ s}^{-1}$ ) obtained from a comparison between the measured and simulated spectra, taking the coupling of 35 Hz between the non-equivalent co-ordinated fluorides into account. The rate constant for acetate dissociation in the ternary complex differs by less than a factor of ten from the one for the binary  $\text{UO}_2(\text{ac})_3^-$  complex discussed below, indicating a similar Eigen–Wilkins type of exchange mechanism.

**In the  $\text{UO}_2(\text{ac})\text{F}_2^-$ ,  $\text{UO}_2(\text{ac})_2\text{F}_2^{2-}$  and  $\text{UO}_2(\text{ac})_2\text{F}^-$  complexes.** The linewidth of the  $^{19}\text{F}$  NMR peak of  $\text{UO}_2(\text{ac})\text{F}_2^-$  is 300 Hz broader than the  $\text{UO}_2(\text{ac})\text{F}_3^{2-}$  peak, but it was not possible to quantify the contributing reactions because fast acetate exchange, water exchange and isomerisation reactions are taking place simultaneously. Different isomers have been observed for the complexes with stronger bonded ligands than acetate, such as oxalate and carbonate.<sup>1</sup> The same increase in line broadening is observed for the saturated  $\text{UO}_2(\text{ac})_2\text{F}_2^{2-}$  complex, where there are two possible isomers that may contribute to the line broadening in addition to the fast acetate exchange. The fluoride peak of  $\text{UO}_2(\text{ac})_2\text{F}^-$  is approximately twice as broad as those of the other complexes,  $k_{\text{obs}} \approx 4000 \text{ s}^{-1}$ . This linewidth is measured at such high acetate concentration that little  $\text{UO}_2(\text{ac})\text{F}$  is present. Hence, this probably does not influence the peak shape. The large linewidth may indicate additional exchange pathways involving co-ordinated water. Six-co-ordination including a co-ordinated water will result in two possible isomers and several exchange pathways.

**Acetate exchange in the binary  $\text{UO}_2(\text{ac})_3^-$  complex.** The investigation was performed in solutions where  $\text{UO}_2(\text{ac})_3^-$  and free acetate are the predominant reactants. From an NMR point of view the system can then be treated as a two-site case. The linewidth of the complex was independent of the concentration of free acetate, indicating exchange *via* the mechanism in eqn. (5). The acetate and uranyl concentrations were varied



at different pH, and by using the known equilibrium data<sup>12</sup> the  $\text{UO}_2(\text{ac})_2$  concentration could be calculated. By plotting  $[\text{UO}_2(\text{ac})_2]$  vs.  $\pi\Delta\nu(\text{ac})$  we found a linear relationship (Fig. 4); in other words, the observed linewidth of the free acetate depends only on the concentration of  $\text{UO}_2(\text{ac})_2$ . The observed rate constant is  $k_{\text{obs}}(\text{ac}) = \pi\Delta\nu(\text{ac}) = k_{-2}[\text{UO}_2(\text{ac})_2]$ , where  $k_{-2} = (3.8 \pm 0.1) \times 10^5 \text{ M}^{-1} \text{ s}^{-1}$  was obtained from the slope of the line. The rate constant for the forward reaction,  $k_1 = (2.75 \pm 0.07) \times 10^3 \text{ s}^{-1}$ , was then calculated from the equilibrium constant for the reaction; this value is in good agreement with  $k_2 \approx 2500 \text{ s}^{-1}$ , calculated from the linewidth of the  $\text{UO}_2(\text{ac})_3^-$  peak. However, this is not suitable for accurate determinations of the rate of exchange because it can only be observed at high total acetate concentrations; at lower concentrations it almost disappears in the baseline, making determination of the linewidth very uncertain.

The effect of protonation on the linewidth of the acetate signal (exchange between Hac and  $\text{ac}^-$ ) was investigated in a separate experiment. Only one exchange averaged signal was observed at different Hac: $\text{ac}^-$  ratios, indicating fast exchange on the timescale determined by the chemical shift difference between the individual species. The data given in Fig. 4 indicate the difficulty in differentiating between the exchange reactions with free acetate and acetic acid. The hydrogen ion concentration could not be varied much; at pH > 5.5 hydrolysed uranyl complexes are formed, while at pH < 4.2 the complex dissociates

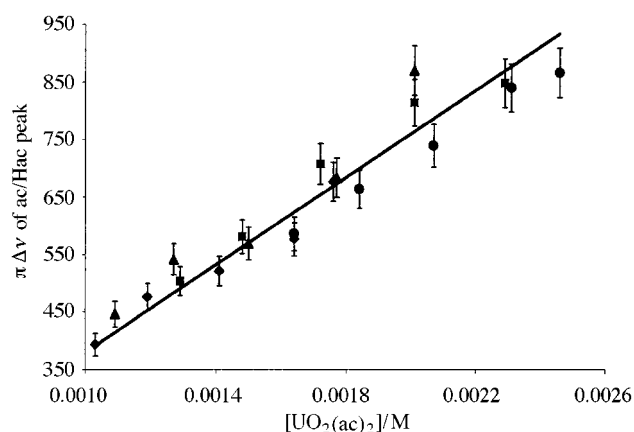
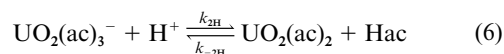


**Fig. 4** Experimental rates of exchange in the uranium(vi)–acetate system, where  $[\text{UO}_2(\text{ac})_2]$ , calculated from Ahrlund and Kullberg,<sup>12</sup> is plotted against the observed line broadening of the free acetate/acetic peak. The bars indicate an experimental uncertainty of 5% in the experimental data. pH 4.57 (●), 4.91 (■), 5.26 (▲) and 5.45 (◆).

(see SUP 57505). At lower pH we have to take the exchange with acetic acid into account, eqn. (6). The observed exchange rate is obtained by summing those of reactions (5) and (6), eqn. (7). Inserting the equilibrium constant  $\beta_{\text{Hac}} = [\text{Hac}]/[\text{ac}^-][\text{H}^+]$  in (7) we obtain eqn. (8) which can be rearranged to (9). The observed rate constant,  $k_{\text{obs}}$ , calculated from the line width of the exchange averaged Hac/ $\text{ac}^-$  acid peak is by definition as in eqn. (10). Combining eqns. (9) and (10) gives (11). By plotting the left side of eqn. (11) against



$$\text{rate} = k_{-2}[\text{UO}_2(\text{ac})_2][\text{ac}^-] + k_{-2\text{H}}[\text{UO}_2(\text{ac})_2][\text{Hac}] \quad (7)$$

$$\text{rate} = k_{-2}[\text{UO}_2(\text{ac})_2][\text{ac}^-] + \beta_{\text{Hac}}k_{-2\text{H}}[\text{UO}_2(\text{ac})_2][\text{ac}^-][\text{H}^+] \quad (8)$$

$$\text{rate}/[\text{UO}_2(\text{ac})_2][\text{ac}^-] = k_{-2} + \beta_{\text{Hac}}k_{-2\text{H}}[\text{H}^+] \quad (9)$$

$$k_{\text{obs}} = \text{rate}/([\text{ac}^-] + [\text{Hac}]) \quad (10)$$

$$k_{\text{obs}}([\text{ac}^-] + [\text{Hac}])/[\text{UO}_2(\text{ac})_2][\text{ac}^-] = k_{-2} + \beta_{\text{Hac}}k_{-2\text{H}}[\text{H}^+] \quad (11)$$

$\beta_{\text{Hac}}[\text{H}^+]$  we obtain (SUP 57505)  $k_{-2} = (4.1 \pm 0.2) \times 10^5 \text{ M}^{-1} \text{ s}^{-1}$  and  $k_{-2\text{H}} = (3.2 \pm 0.4) \times 10^5 \text{ M}^{-1} \text{ s}^{-1}$ . The rate constant for the proton assisted dissociation of acetic acid in eqn. (6),  $k_{2\text{H}} = 9 \times 10^7 \text{ M}^{-1} \text{ s}^{-1}$ , was calculated using the known equilibrium constant for reaction (6). It is four orders of magnitude larger than that for the non-protonated pathway,  $k_2$ .

The activation parameters for the reverse reaction in eqn. (5) were determined from the temperature dependence of the linewidth of the acetate peak. From a least-squares fitting of the experimental rate constants using the Eyring equation (SUP 57505) the following activation parameters were calculated,  $\Delta S^\ddagger = -61 \pm 9 \text{ J K}^{-1} \text{ mol}^{-1}$  and  $\Delta H^\ddagger = 22 \pm 3 \text{ kJ mol}^{-1}$ .

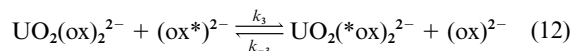
The kinetics of the complex formation/dissociation in the binary uranium(vi)–acetate system has previously been studied by Hurwitz and Kustin<sup>15</sup> using the temperature-jump technique. They found a rate constant of  $2 \text{ s}^{-1}$  for the acetate dissociation in the  $\text{UO}_2(\text{ac})_3^-$  complex, which is three orders of magnitude slower than that determined here. This rate constant is not compatible with the  $^{13}\text{C}$  NMR data.

#### Oxalate exchange in the binary $\text{UO}_2(\text{ox})_2^{2-}$ complex

Two different modes of co-ordination of oxalate<sup>16,17</sup> have been found in solids containing  $\text{UO}_2(\text{ox})_3^{4-}$ . Two oxalate ions are always chelated, while the third can be bonded either bidentate

with one of the carboxylate groups,<sup>17</sup> giving six-co-ordination in the equatorial plane or unidentate with only one oxygen,<sup>16</sup> giving five-co-ordination. The small value of  $\log K_3 = 0.54$  for the binary oxalate system means that  $\text{UO}_2(\text{ox})_2^{2-}$  is the predominant complex even at rather high oxalate concentrations, and the NMR methodology had to be modified accordingly, as described in more detail below and in Scheme 2.

The exchange between  $\text{UO}_2(\text{ox})_2^{2-}$  and free oxalate was studied using their  $^{13}\text{C}$  NMR signals, in much the same way as in the acetate system. The test solutions contained 5 mM  $\text{U}^{\text{VI}}$  at pH 7.3, and the total oxalate concentration was varied between 20 and 50 mM at  $-5^\circ\text{C}$ , where mainly  $\text{UO}_2(\text{ox})_2^{2-}$  and oxalate are present. As in the acetate system, a linear relationship was found between the line broadening of the  $\text{UO}_2(\text{ox})_2^{2-}$  peak and the equilibrium concentration of free oxalate (SUP 57505). The exchange reaction, without any net chemical exchange, is consistent with these results, eqn. (12). A least-squares linear



analysis of the experimental data gave  $2k_3 = (3.21 \pm 0.05) \times 10^3 \text{ M}^{-1} \text{ s}^{-1}$ , where the factor 2 takes the reverse reaction into account. The rate of oxalate exchange was independent of the hydrogen ion concentration, as observed both by measuring the line broadening and magnetisation transfer experiments in the pH range 2–7. The activation parameters,  $\Delta S^\ddagger = -56 \pm 5 \text{ J K}^{-1} \text{ mol}^{-1}$  and  $\Delta H^\ddagger = 31 \pm 2 \text{ kJ mol}^{-1}$ , were determined from the temperature dependence of the linewidths at pH 6.9. The Eyring plot is given in SUP 57505.

The activation parameters for the exchange between  $\text{UO}_2\text{L}_2(\text{H}_2\text{O})$  and L, for L = oxalate and acetate, are of the same order of magnitude, indicating similar Eigen–Wilkins<sup>18</sup> type of exchange mechanisms, where the first step is the formation of an outer sphere complex ( $K_{\text{os}}$ ) followed by the rate determining dissociation of water ( $k_{\text{aq}}$ ) as shown in Scheme 2. The observed rate is then  $k_{\text{obs}} = K_{\text{os}}k_{\text{aq}}$ . Concerted reactions of this type have been suggested in some previous studies of exchange reactions of uranium(VI) chelates<sup>19–21</sup> and the binary uranyl fluoride system.<sup>1</sup> By using  $K_{\text{os}} = 0.3$  and  $1.1 \times 10^{-3} \text{ M}$  calculated from the Fuoss equation<sup>22</sup> the rate constant for the water exchange at  $-5^\circ\text{C}$  is equal to  $1.3 \times 10^6$  and  $2.9 \times 10^6 \text{ s}^{-1}$  in the acetate and oxalate system respectively. These values are close to that calculated for the exchange of water in  $\text{UO}_2(\text{H}_2\text{O})_5^{2+}$ , as measured by  $^{17}\text{O}$  NMR at the same temperature ( $4.1 \times 10^5 \text{ s}^{-1}$ ). These results will be described in a forthcoming paper.<sup>23</sup>

#### Oxalate exchange in the ternary $\text{UO}_2(\text{ox})_2\text{F}^{3-}$ complex

The rate constant for the oxalate exchange<sup>3</sup> in the saturated ternary  $\text{UO}_2(\text{ox})_2\text{F}^{3-}$  complex is independent of the concen-

trations of fluoride and oxalate, and first order in the concentration of the complex, indicating an oxalate attack after the rate determining step. We have suggested<sup>3</sup> that oxalate exchange takes place along two parallel pathways. One of the mechanisms has first a fluoride dissociation, followed by a slower ring opening/exchange of co-ordinated oxalate. In this reaction  $\text{UO}_2(\text{ox})_2^{2-}$  or  $\text{UO}_2(\text{ox})_2(\text{H}_2\text{O})^{2-}$  is an intermediate. From information on the exchange mechanisms of the binary oxalate system we know that the oxalate exchange in  $\text{UO}_2(\text{ox})_2(\text{H}_2\text{O})^{2-}$  follows a second order rate law, which rules out this as an intermediate in the ternary system.

#### Proton catalysis in the ligand exchange reactions

One expects that the proton catalysed ligand exchange reactions will depend strongly on the site of the proton attack. Proton binding in the acetate case must take place at a co-ordinated carboxylate oxygen; this is not necessary in the ternary oxalate and carbonate systems, where there are non-co-ordinated oxygen sites available. The catalytic effect is expected to be much larger in the first case than in the second. In the same way the catalytic effect in the binary systems is expected to be larger for acetate than for oxalate, as observed experimentally. The

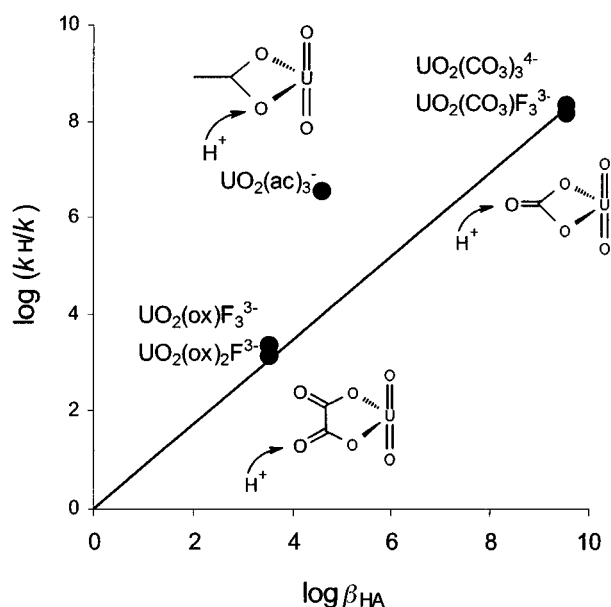
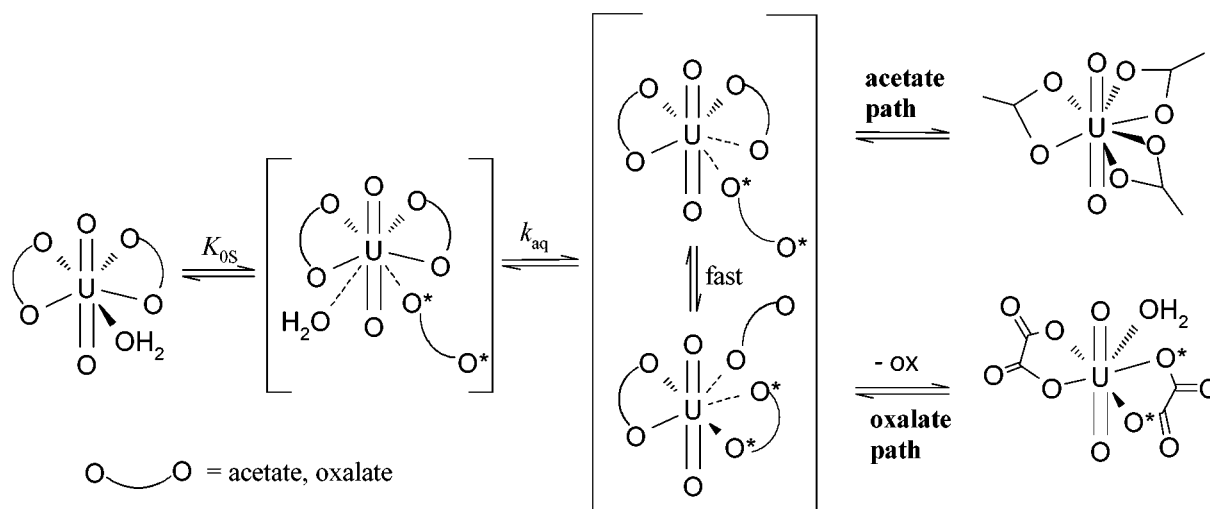


Fig. 5 A linear free energy relationship illustrating the relation between the catalytic effect of  $\text{H}^+$  and the protonation constant of the ligand; data for binary<sup>24</sup> and ternary carbonate<sup>2</sup> and ternary oxalate<sup>3</sup> are taken from the literature.



Scheme 2

$\text{H}^+/\text{D}^+$  isotope effects of the catalysed reactions have been studied for the  $\text{UO}_2(\text{ox})_2\text{F}^{3-}$  and  $\text{UO}_2(\text{CO}_3)_3^{4-}$  complexes,<sup>3,24</sup> and both are more effectively catalysed by  $\text{D}^+$  than  $\text{H}^+$ . This is a clear indication of the formation of a precursor before the ligand exchange. Hence, one expects a linear free energy relationship between the proton affinity of the ligand and the catalytic effect. The  $\log K$  for protonation of the ligand is a measure of the proton affinity, and  $\log (k_{\text{H}}/k)$ , where  $k_{\text{H}}$  and  $k$  are the rate constants for the proton catalysed and non-catalysed pathways is a measure of the catalytic effect. Fig. 5 shows the correlation between these quantities. For the oxalate and carbonate complexes there is a clear correlation between the basicity of the ligand and the catalytic effect. The data for the acetate system lie above the straight line as expected, because the proton attack takes place on a co-ordinated carboxylate oxygen.

## Acknowledgements

This study has been supported by grants from the Franz-Georg and Gull Liljenroth Foundation and by the Swedish Nuclear Fuel and Waste management Co (SKB).

## References

- 1 Z. Szabó, J. Glaser and I. Grenthe, *Inorg. Chem.*, 1996, **35**, 2036.
- 2 Z. Szabó, W. Aas and I. Grenthe, *Inorg. Chem.*, 1997, **36**, 5369.
- 3 Z. Szabó and I. Grenthe, *Inorg. Chem.*, 1998, **37**, 6214.
- 4 M. Harada, Y. Fujii, S. Sakamaki and H. Tomiyasu, *Bull. Chem. Soc. Jpn.*, 1992, **65**, 3022.
- 5 W. Aas, A. Moukhamet-Galeev and I. Grenthe, *Radiochim. Acta*, 1998, **82**, 77.
- 6 L. Ciavatta, D. Ferri, I. Grenthe and F. Salvatore, *Inorg. Chem.*, 1981, **20**, 463.
- 7 H. M. Irving, M. G. Miles and L. D. Pettit, *Anal. Chim. Acta*, 1967, **38**, 475.
- 8 A. Liberti and M. Mascini, *Anal. Chem.*, 1969, **41**, 676.
- 9 L. G. Sillén and B. Warnquist, *Ark. Kemi*, 1969, **31**, 315.
- 10 A. L. V. Geet, *Anal. Chem.*, 1970, **42**, 679.
- 11 Z. Szabó and J. Glaser, *Magn. Reson. Chem.*, 1995, **33**, 20.
- 12 S. Åhrland and L. Kullberg, *Acta Chem. Scand.*, 1971, **25**, 3677.
- 13 S. Åhrland and L. Kullberg, *Acta Chem. Scand.*, 1971, **25**, 3457.
- 14 W. H. Zachariasen and H. A. Plettinger, *Acta Crystallogr., Sect. C*, 1959, **12**, 526.
- 15 P. Hurwitz and K. Kustin, *J. Phys. Chem.*, 1967, **71**, 324.
- 16 N. W. Alcock, *J. Chem. Soc., Dalton Trans.*, 1973, 1614.
- 17 N. W. Alcock, *J. Chem. Soc., Dalton Trans.*, 1973, 1610.
- 18 M. Eigen and R. G. Wilkins, *Adv. Chem. Ser.*, 1965, **49**, 55.
- 19 Y. Ikeda, H. Tomiyasu and H. Fukutomi, *Bull. Chem. Soc. Jpn.*, 1984, **57**, 2925.
- 20 L. Rodehüser, P. R. Rubini, K. Bokolo and J.-J. Delpuech, *Inorg. Chem.*, 1982, **21**, 1061.
- 21 Y. Ikeda, H. Tomiyasu and H. Fukutomi, *Bull. Chem. Soc. Jpn.*, 1983, **56**, 1060.
- 22 R. M. Fouss, *J. Am. Chem. Soc.*, 1958, **80**, 5050.
- 23 I. Bányai, I. Farkas, I. Grenthe and Z. Szabó, in preparation.
- 24 I. Bányai, J. Glaser, K. Micskei, I. Tóth and L. Zékány, *Inorg. Chem.*, 1995, **34**, 3785.

Paper 8/08416E

